# Anionic Living Polymerization of Macromonomers: Preparation of $(A)_n$-*star*-$(B)_1$ Star Block Copolymers and Some Properties of the Products Obtained

**Kazunori Se* and Yasunari Hayashino**

*Department of Materials Science and Engineering, Faculty of Engineering, Fukui University, Bunkyo 3-9-1, Fukui 910-8507, Japan*

*Received August 12, 2006; Revised Manuscript Received November 23, 2006*

ABSTRACT: (4-Vinylbenzyl)polystyrene macromonomer (PStM, $M_n = 5.4_5 \times 10^3$, $M_w/M_n = 1.0_3$) was living-anionically polymerized by *sec*-BuLi to produce the $(PSt)_n^-$ star polymer under high vacuum at room temperature. Then, isoprene (Is) was sequentially copolymerized by $(PSt)_n^-$ to yield the $(PSt)_{6.1}$-*s*-$(PIs)_1$ star block copolymer ($M_n = 6.3_9 \times 10^4$, $M_w/M_n = 1.0_4$) having a narrow PIs composition distribution. Similarly, the $(PIs)_{6.6}$-*s*-$(PSt)_1$ star block copolymer ($M_n = 10._8 \times 10^4$, $M_w/M_n = 1.0_4$) was prepared using (4-vinylbenzyl)polyisoprene macromonomer (PIsM, $M_n = 5.1_9 \times 10^3$, $M_w/M_n = 1.0_4$). The synthetic route by which the $PIs^-$ carbanions copolymerize PStM was found to be unsuitable for preparing $(PIs)_1$-*star*-$(PSt)_n$. The resultant star polymers and star block copolymers were characterized by a special analysis using a gel permeation chromatograph equipped with a low-angle laser light-scattering detector. The living mechanism of the macromonomers polymerization was discussed from the viewpoint of initiation efficiency. The asymmetric architecture of the resultant samples was also discussed on the basis of the relationship between molecular weights and molecular dimensions using a model of regular comb-shaped polymers. Two films of the $(A)_n$-*star*-$(B)_1$ star block copolymers showed a clear microphase-separated structure as observed by transmission electron microscopy. Their morphologies shifted to the higher star polymer content side of the morphological transition line for linear block copolymers. This interesting gap in the morphology between the star block copolymers and linear block copolymers was quantitatively explained by a volume fraction and an asymmetric factor.

## Introduction

Nonlinear block copolymers, such as mikto-arm star block copolymers,[1] block-graft copolymers,[2,3] and rod−coil linear block copolymers,[4] exhibit unique microphase separation behavior because of their asymmetric architecture.[5] In particular, an ABC-type mikto-arm star block copolymer with three mutually immiscible blocks can offer a great deal of design flexibility for the formation of new types of microphase-separated structures.[6,7] To prepare these nonlinear block copolymers, sophisticated synthetic routes might be required, and the final products yields might be small.

On the other hand, poly(macromonomer)s (abbreviated as poly$(A)_p$) can be prepared by radical polymerization of the corresponding macromonomers, and they show unique physical properties, such as liquid crystalline[8] and anisotropic solution properties,[9] that are different from those of linear polymers and star polymers. The molecular architecture of poly$(A)_p$ can be considered identical to that of comblike polymers when the degree of polymerization of the macromonomer ($p$) is large.[10] It has been known that the A arm chain of the $(A)_q$ star polymers extends much father than the corresponding unperturbed polymer chain of the A linear polymer. Furthermore, the A chain of poly$(A)_p$ might extend much father than the corresponding A chain of the $(A)_q$ star polymers when $p > q$ because the A comb chain in poly$(A)_p$ becomes much more crowded near the grafting points than the A arm chain in $(A)_q$.[9,10] By combining these two effects, namely, an ABC-type mikto-arm star block copolymer and the presence of star polymers with many arms as in the case of poly$(A)_p$, the $(A)_n$-*star*-$(B)_m$-*star*-$(C)_r$ star block copolymers should form many more microphase-separated structures than the corresponding ABC-type mikto-arm star block copolymers.

In order to prepare the $(A)_n$-*star*-$(B)_m$-*star*-$(C)_r$ star block copolymers in sufficient quantities, simpler, more general synthetic routes than those reported thus far are needed. Anionic living polymerization of macromonomers[11−18] is one of the synthetic routes expected to be useful for preparing the $(A)_n$-*star*-$(B)_m$-*star*-$(C)_r$ star block copolymers having a narrow molecular weight distribution and a narrow composition distribution. Purification of macromonomers is one of the major problems encountered in their anionic living polymerization. We previously prepared a particle-like purging reagent and showed that it was useful for purifying the macromonomers, and its effect was described elsewhere.[18]

Before presenting the preparation of the $(A)_n$-*star*-$(B)_m$-*star*-$(C)_r$ star block copolymers, the present paper describes the synthesis of the $(A)_n$-*star*-$(B)_1$ star block copolymers by anionic living polymerization of two macromonomers. Because initiation efficiency is one of the most important characteristics of living mechanisms, we consider this value at length in our present preparation of $(A)_n$-*star*-$(B)_1$ star block copolymers. The asymmetric architecture of the $(A)_n$-*star*-$(B)_1$ is discussed on the basis of the relationship between molecular weight and molecular dimension. The microphase-separated structure of the $(A)_n$-*star*-$(B)_1$ star block copolymers is also discussed from the viewpoint of a volume fraction and an asymmetric factor that corresponds to the ratio of the number of arms of A chains to the number of arms of B chains.

## Experimental Section

**Reagents.** *sec*-Butyllithium (*sec*-BuLi) was purchased and diluted with purified *n*-heptane. The concentration of the initiator was

* Corresponding author: Tel +81-776-27-8957; Fax +81-776-27-8767; e-mail se@matse.fukui-u.ac.jp.

10.1021/ma061849o CCC: $37.00 
Published on Web 01/06/2007

**Table 1. Molecular Characteristics of Polystyrene Macromonomer (PStM) and Polyisoprene Macromonomer (PIsM)**

| macromonomers | $10^{-3}M_n$[a] GPC and VPO | $M_w/M_n$[a] GPC | $f_c$[b] |
|---|---|---|---|
| PStM | $5.4_5$ | $1.0_3$ | 1.00 |
| PIsM | $5.1_9$[c] | $1.0_4$ | 0.95 |

[a] Determined by GPC using standard PSts, by GPC-LALLS, and by VPO. [b] Coupling efficiency determined by $M_n/M_n^{NMR}$. [c] Determined using $M_n = 2.3_1(M_n^{GPC})^{0.86} = 2.3_1(7.8_9 \times 10^3)^{0.86} = 5.1_9 \times 10^3$, where $M_n^{GPC}$ was determined by GPC using standard PSts.

determined by titration with a standard HCl solution. Styrene (St), isoprene (Is), and α-methylstyrene were dried over calcium hydride under a pressure of $10^{-6}$ mmHg and purified with octylbenzophenone sodium.[19,20] 4-Vinylbenzyl chloride (4VBC) was prepared through a common method previously used by the present authors.[18] The resultant 4VBC was dried over calcium hydride several times under a pressure of $10^{-6}$ mmHg.

The toluene and benzene used for polymerization and the *n*-heptane used for dilution of the initiator were dried with sodium metal, distilled in a vacuum with sodium metal, and then purified by distillation from a mixture of 1,1-diphenylhexyllithium (toluene and benzene) and *n*-butyllithium (*n*-heptane). The tetrahydrofuran (THF) used for preparation of the macromonomers was dried with sodium metal, distilled in a vacuum with anthracene sodium, and then purified by distillation from a mixture of α-methylstyrene tetramer−sodium.

**Macromonomers.** (4-Vinylbenzyl)polystyrene macromonomer (PStM) was prepared as described previously.[18] Isoprene was anionically polymerized by *sec*-BuLi in toluene at room temperature under a pressure of $10^{-6}$ mmHg, and α-methylstyrene ([α-methylstyrene]/[*sec*-BuLi] = 2.5) was added to the solution at 50 °C above the ceiling temperature of α-methylstyrene to change the living end of polyisoprene (PIs) from isoprenyllithium to α-methylstyryllithium. The degree of end-functionalization was determined by comparing relative $^1$H NMR intensities between two $CH_3$ groups (0.85 ppm) of the *sec*-butyl initiator residue and a phenyl group (7.15−7.30 ppm) of the α-methylstyrene residue. The degree of the end-functionalization was $1.5_2$. Then, the polymerization solution was kept at −78 °C and was changed to a mixture of toluene/THF (1/1 v/v) by adding THF. Finally, a THF solution of 4VBC ([4VBC]/[*sec*-BuLi] = 2.5) was added to the polymerization solution at −78 °C to prepare (4-vinylbenzyl)polyisoprene macromonomer (PIsM).

The coupling efficiency ($f_c$) was determined by the following two methods. (1) $M_n^{NMR}$ was determined from the ratio of the relative $^1$H NMR intensities of polystyrene or polyisoprene to a $CH_2$═C group (5.7 and 6.7 ppm) introduced into a chain end, and $M_n$ was determined by means of a gel permeation chromatograph (GPC) equipped with a low-angle laser light-scattering (GPC-LALLS) detector and/or by vapor pressure osmometry. The $f_c$ value was determined by $M_n/M_n^{NMR}$. (2) The $f_c$ value was also determined by comparing the relative $^1$H NMR intensities between the two $CH_3$ groups (0.55−0.80 ppm) of the *sec*-butyl group at a chain end and a $CH_2$═C group introduced at the other chain end.[21] The two $f_c$ values were coincident with each other with an error of less than 1%. The molecular characteristics and the $f_c$ values of the PStM and PIsM macromonomers are described in Table 1.

**Purification of the Macromonomers.** The PStM and PIsM macromonomers were purified by the same method as follows. The macromonomers were dissolved in THF and precipitated in excess methanol to remove the 4VBC, which was not reacted with polystyryllithium and polyisopreny α-methylstyryllithium. After drying under a high vacuum, each of the Bz solutions of the resultant macromonomers was introduced to an ampule with a break-seal, freeze-dried under a vacuum for 10 h, and sealed off by flame. The freeze-dried macromonomers were further dried under a pressure of $10^{-6}$ mmHg for 72 h, added to new Bz, and sealed off by flame.

A purging reagent for precisely purifying the macromonomers was prepared; this was a cross-linked polystyrene particle containing

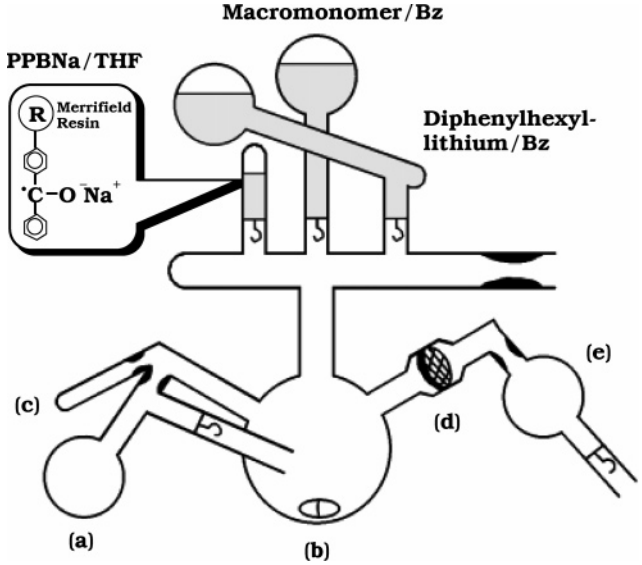


**Figure 1.** A glass reactor for purification of PStM and PIsM macromonomers using PPBNa. The symbols of (a)−(e) are explained in the text.

a benzophenone sodium complex ($R-C_6H_4-CO^-C_6H_5Na^+$, PPBNa). PPBNa was prepared from a cross-linked polystyrene particle containing divinylbenzene (Merrifield resin,[22] $R-C_6H_5$) via the following synthetic routes.

$$R-C_6H_5 + C_6H_5COCl \rightarrow R-C_6H_4-COC_6H_5 \quad (1)$$

$$R-C_6H_4-COC_6H_5 + Na \rightarrow R-C_6H_4-CO^-C_6H_5Na^+ \quad (2)$$

The PPBNa was found to have a sodium content of 8.1 wt %, and the metalation efficiency per one styrene unit was 67%. The PPBNa was found to work as a purging reagent for the monomers and macromonomers employed in the anionic living polymerization. The details of the preparation and purging characteristics of PPBNa have been reported elsewhere.[18]

The dried macromonomers were purified in a sealed glass apparatus (Figure 1) by a special procedure using PPBNa as follows. The inside of the glass apparatus was washed with Bz solution of 1,1-diphenylhexyllithium, and the Bz solution was collected in an ampule (a) and then sealed off by flame. The PPBNa suspended in THF was introduced into a glass reactor (b), the THF was distilled in an ampule (c) kept in liquid nitrogen, and the ampule was sealed off by flame. Then, the Bz solution of the macromonomers was introduced into the reactor (b), and the suspended mixture was stirred at room temperature for 3−10 h. The Bz solution of the macromonomer was then separated from the suspension by a glass filter (d) and was introduced into an ampule (e). A part of the resultant macromonomer was checked to see whether or not the macromonomer had become a poly(macromonomer) during purification. The resultant macromonomers were anionically polymerized.

**Polymerization.** The $(A)_n$ star polymers and $(A)_n$-*star*-$(B)_1$ star block copolymers were prepared using an anionic living polymerization technique. Polymerization was carried out in a sealed glass apparatus under a pressure of $10^{-6}$ mmHg. The polymerization techniques were almost the same as those employed in previous studies conducted by the present authors.[19,20]

**Molecular Characterization.** The number-average molecular weights ($M_n$) of the two macromonomers were determined by vapor pressure osmometry (VPO; model 117, Hitachi, Tokyo, Japan) in Bz at 30 °C and by means of a GPC (model CCPD, Tosoh Co., Tokyo, Japan). Molecular characterization of all samples was carried out in THF using a GPC equipped with a low-angle laser light-scattering (GPC-LALLS) detector (model LS-8000, Tosoh Co.) and RI detector (RI-8010, Tosoh Co.). For the GPC measurements, four

**Table 2. Preparation of $(A)_n$-*star*-$(B)_1$ Star Block Copolymers**

| polymers[a] | first monomer (g) | second monomer (g) | *sec*-BuLi ($10^{-4}$ mol) | polym time (h) | Bz (mL) | $10^{-3}M_k$ |
|---|---|---|---|---|---|---|
| $(PSt)_{6.1}$-*s*-$(PIs)_1$ | $2.8_6$ | $2.5_5$ | $1.4_2$ | 60 | 70 | $(5.4_5)_{3.7}$-*s*-$(17._9)_1$ |
| $(PIs)_{6.6}$-*s*-$(PSt)_1$ | 0.70 | $1.4_9$ | 0.75 | 17 | 30 | $(5.1_9)_{1.8}$-*s*-$(19._9)_1$ |
| $(PIs)_1$-*s*-$(PSt)_{11}$ | $2.5_0$ | $2.5_3$ | $1.4_7$ | 70 | 70 | $(17._0)_1$-*s*-$(5.4_5)_{3.2}$ |

[a] PStM and PIsM macromonomers were polymerized to prepare the $(PSt)_n$ and $(PIs)_n$ star polymers, respectively.

high-resolution columns (G2500H, G3000H, G400H, and GMH-M, 7.8 mm × 60 cm; Tosoh Co.) were connected in a series.

A special analysis was required to determine $M_n$ and $M_w$ values of the star block copolymers using GPC-LALLS.[23] This is because the star block copolymers have a molecular weight distribution and a composition distribution (CD) among the different molecular weight and the same molecular weights. For this reason, we will consider the molecular weight, the refractive index increment, and the concentration of the star block copolymer at the *i*th elution volume as $M_{i,j}$, $(dn/dc)_{i,j}$, and $C_{i,j}$, respectively. That is, a molecular weight distribution can be represented by the subscript *i*, and the CD can be represented by the subscript *j*. Thus, the refractive index (RI) intensity ($H_i^{RI}$) and the LALLS intensity ($H_i^{LS}$) of the corresponding RI and LALLS chromatograms of the block copolymers at the *i*th elution volume can be described as follows.

$$H_i^{RI} = k_{RI}\sum_j (dn/dc)_{i,j}C_{i,j} \tag{3}$$

$$H_i^{LS} = k_{LS}\sum_j [(dn/dc)_{i,j}]^2 M_{i,j}C_{i,j} \tag{4}$$

As a first approximation, one can assume that $M_{i,j} = M_i$ because the polymer chains having $M_{i,j}$ appeared at the same *i*th elution volume. As reported by the present authors elsewhere, the $M_n^{LALLS}$ values determined using $M_{i,j} = M_i$ were found to be equal to the $M_n^{OSM}$ values determined by membrane osmometry for linear and star block copolymers.[23] The relation of $M_{i,j} = M_i$ is an assumption but was found to be used for determining $M_n^{LALLS}$ of the star block copolymers having sharp composition distributions in THF as a good solvent for PSt and PIs. Therefore, $M_{i,j}$ in eq 4 can be changed to $M_i$ and moved outside of the summation of $\sum_j$. By this treatment, when $a = b$ in eq 3 and $c = d$ in eq 4, $a^2/c = b^2/d$ can hold. From the $a^2/c = b^2/d$, eq 5 can be derived as follows:

$$M_i = \frac{(k_{RI})^2}{k_{LS}}\frac{H_i^{LS}}{(H_i^{RI})^2}\frac{[\sum_j (dn/dc)_{i,j}C_{i,j}]^2}{\sum_j [(dn/dc)_{i,j}]^2 C_{i,j}} \tag{5}$$

With the relation of $\sum_j C_{i,j} = C_i$ in mind, the two summations in eq 5 can be changed as follows: $\sum_j (dn/dc)_{i,j}C_{i,j} = C_i\langle(dn/dc)_{i,j}\rangle = C_i(dn/dc)_i$ and $\sum_j [(dn/dc)_{i,j}]^2 C_{i,j} = C_i\langle[(dn/dc)_{i,j}]^2\rangle = C_i[(dn/dc)_i]^2$, where $\langle ... \rangle$ means the average of the corresponding refractive index increments. The corresponding equations of $M_i$ thus become

$$M_i = [(k_{RI})^2/k_{LS}](H_i^{LS}/(H_i^{RI})^2)C_i \tag{6}$$

By substituting $M_i$ in $M_n = \sum H_i^{RI}/\sum(H_i^{RI}/M_i)$ and $M_w = \sum H_i^{RI}M_i/\sum H_i^{RI}$, the corresponding values of $M_n^{LALLS}$ and $M_w^{LALLS}$ were calculated.[23]

On the other hand, the PIs weight fraction of $(PSt)_n$-*star*-$(PIs)_1$ star block copolymers at the *i*th elution volume of the GPC chromatogram can be determined as[24]

$$w_i^{PIs} = \frac{\epsilon_{PSt}H_i^{RI} - k^{RI}_{PSt}H_i^{UV}}{(\epsilon_{PSt} - \epsilon_{PIs})H_i^{RI} + (k^{RI}_{PIs} - k^{RI}_{PSt})H_i^{UV}} \tag{7}$$

where $H_i^{RI}$ and $H_i^{UV}$ are the RI intensity and UV intensity, and $\epsilon_{PSt}$, $k^{RI}_{PSt}$, $\epsilon_{PIs}$, and $k^{RI}_{PIs}$ are instrumental constants that were previously determined by the GPC measurements of PSt and PIs using a UV detector (UV-8011, Tosoh Co.) and an RI detector.

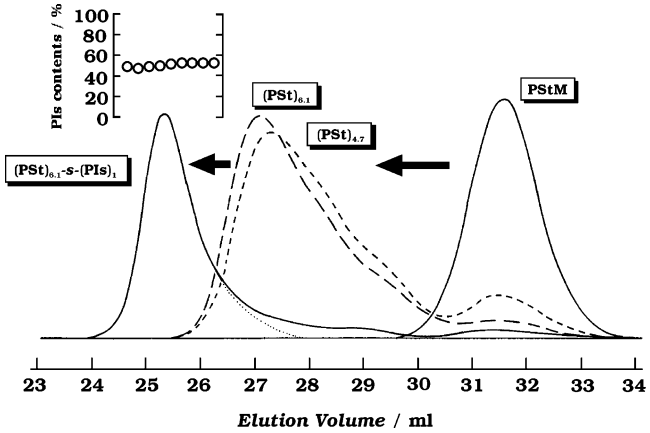


**Figure 2.** GPC chromatograms of $(PSt)_n$ star polymers and $(PSt)_{6.1}$-*s*-$(PIs)_1$ star block copolymer. The final product was purified by repeated dissolution−reprecepitation, and the resultant GPC chromatogram of $(PSt)_{6.1}$-*s*-$(PIs)_1$ is also shown as a broken curve.

**Transmission Electron Microscopy.** Star block copolymers were cast from 5% w/w THF solution into thin films of ~0.5 mm thickness by gradually evaporating solvent at 25 °C. THF is a good solvent for the two constituent polymers. The resultant films were completely dried under a reduced pressure of $10^{-3}$ mmHg at 40 °C. The films were stained with a fixing reagent of osmium tetraoxide ($OsO_4$), embedded in a resin, and cut into ultrathin sections by an ultramicrotome. The morphology of these sections was examined using a Hitachi type H-7500 transmission electron microscope.

## Results and Discussion

**Preparation of Star Block Copolymers of $(A)_n$-*star*-$(B)_1$.** In this section, the first approach is discussed, namely, the polymerization of macromonomers followed by copolymerization of the corresponding monomers. The two synthetic routes using PStM and PIsM macromonomers are as follows, and the polymerization conditions are shown in Table 2.

$$n\text{PStM} + s\text{-BuLi} \rightarrow (PSt)_n^- \tag{8}$$

$$(PSt)_n^- + \text{Is} \rightarrow (PSt)_n\text{-}star\text{-}(PIs)_1 \tag{9}$$

$$n\text{PIsM} + s\text{-BuLi} \rightarrow (PIs)_n^- \tag{10}$$

$$(PIs)_n^- + \text{St} \rightarrow (PIs)_n\text{-}star\text{-}(PSt)_1 \tag{11}$$

In eq 8, when the Bz solution of PStM was introduced into the heptane solution of the *s*-BuLi initiator, the polymerization solution changed for a few seconds from colorless to red, a characteristic color of carbanions. The solutions maintained a red color during the homopolymerization of PStM. As shown in Figure 2, with an increase in polymerization time from 0.4 to 4.6 h, the GPC peak strength of PStM decreased, and at the same time, the GPC peaks of the corresponding $(PSt)_n$ star polymers shifted to the higher $M_n$ sides and their peak strength increased. As shown in Table 3, the $M_n$ values of $(PSt)_n$

**Table 3. Molecular Characteristics of $(PSt)_n$ Star Polymers[a] and $(PSt)_n$-*s*-$(PIs)_1$ Star Block Copolymer[a]**

| | | $10^{-4}M_n$ | | $M_w/M_n$ | | | | | $w^{PIs}$/%[e] | |
|---|---|---|---|---|---|---|---|---|---|---|
| polymers | *t* (h) | GPC | LALLS[b] | GPC | LALLS[b] | arms[c] | yield/% PStM | $f_I$[d] | $M_n$ | $\sum w_i^{PIs}$ |
| $(PSt)_{4.7}$ | 0.4 | $1.6_8$ | $2.5_8$ | $1.1_6$ | $1.2_5$ | 4.7 | 81 | 0.62 | | |
| $(PSt)_{5.8}$ | 1.4 | $1.7_2$ | $3.1_9$ | $1.1_3$ | $1.1_6$ | 5.8 | 95 | 0.60 | | |
| $(PSt)_{5.9}$ | 3.0 | $1.7_3$ | $3.2_3$ | $1.1_2$ | $1.1_5$ | 5.9 | 97 | 0.60 | | |
| $(PSt)_{6.1}$ | 4.6 | $1.7_9$ | $3.3_3$ | $1.1_0$ | $1.1_3$ | 6.1 | 100 | 0.60 | | |
| $(PSt)_{6.1}$-*s*-$(PIs)_1$[f] | 60 | $4.7_2$ | $6.3_9$ | $1.0_5$ | $1.0_4$ | | 100[g] | 1.00[g] | 48 | 50 |

[a] Prepared by *sec*-BuLi in Bz at room temperature under a pressure of $10^{-6}$ mmHg. [b] A special analysis using GPC equipped with low-angle laser light scattering.[23] [c] The degree of polymerization of the $(PSt)_n$ star polymers. [d] Initiation efficiency determined by $M_n/M_n$. [e] PIs contents determined by $M_n^{PIs}/M_n^{block}$ and by GPC using UV and RI detectors. [f] $M_n = (5.4_5 \times 10^3\ g\ mol^{-1}) \times 6.1_1 + (3.0_6 \times 10^4\ g\ mol^{-1}) = 6.3_9 \times 10^4\ g\ mol^{-1}$. [g] Determined for the second monomer of Is.

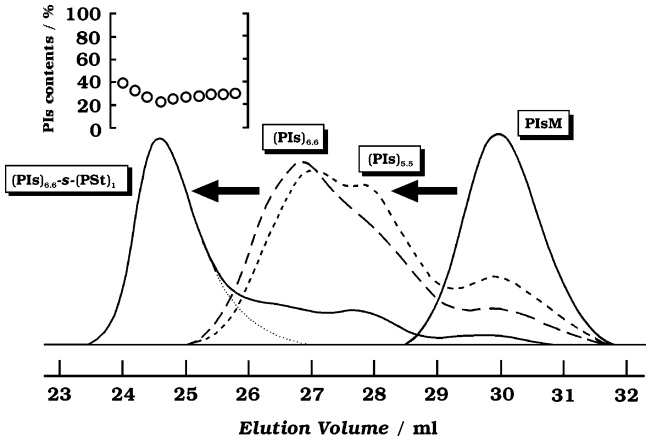


**Figure 3.** GPC chromatograms of $(PIs)_n$ star polymers and $(PIs)_{6.6}$-*s*-$(PSt)_1$ star block copolymer. The final product was purified by repeated dissolution−reprecepitation, and the resultant GPC chromatogram of $(PIs)_{6.6}$-*s*-$(PSt)_1$ is also shown as a broken curve.

increased linearly with an increase in the $(PSt)_n$ yields, and finally, the number of arms for the $(PSt)_n$ star polymer reached 6.1 as calculated by the ratio of $M_n$ of $(PSt)_n$ to the $M_n$ of PStM, assuming a PStM consumption of 100%. The $M_w/M_n$ values are close to 1.1. These behaviors suggest that the polymerization of the PStM macromonomer is "living".

When Is was introduced into the $(PSt)_{6.1}^-$ polymerization solution, the solution gradually changed to yellow. A GPC peak of $(PSt)_{6.1}$-*star*-$(PIs)_1$ appeared at the higher $M_n$ side at an Is consumption of 100%. The PIs weight fraction of the resultant $(PSt)_{6.1}$-*star*-$(PIs)_1$ star block copolymer was calculated to be 48% by means of the ratio $M_n$ of PIs/$M_n$ of $(PSt)_n$-*star*-$(PIs)_1$ and to be 50% by the ratio $\sum_j(H_i^{RI}w_i^{PIs})/\sum_j H_i^{RI}$ in eq 7, which is close to the feed ratio of 47% that was calculated using Is of $2.5_5$ g and PStM of $2.8_6$ g. The PIs composition distribution against the elution volume was found to be narrow, as shown in Figure 2. We succeeded in preparing a $(PSt)_{6.1}$-*star*-$(PIs)_1$ star block copolymer having a narrow molecular weight distribution and a narrow composition distribution by anionic living polymerization of the PStM macromonomer.

By a process of eq 10 similar to that described in eq 8, the PIsM macromonomer was anionically polymerized by *s*-BuLi to produce $(PIs)_n$ star polymers. As shown in Figure 3 and Table 4, the $M_n$ values of $(PIs)_n$ increased linearly with an increase in the $(PIs)_n$ yields, and finally, the number of arms for the $(PIs)_n$ star polymer reached 6.6, as calculated using the ratio of the $M_n$ of $(PIs)_n$ to the $M_n$ of PIsM assuming a 100% PIsM consumption. The $M_w/M_n$ values were close to 1.04. When St was introduced into the $(PIs)_n^-$ polymerization solution, a GPC peak of $(PIs)_{6.6}$-*star*-$(PSt)_1$ appeared at the higher $M_n$ side. The PIs weight fraction of the resultant $(PIs)_{6.6}$-*star*-$(PSt)_1$ star block copolymer was calculated to be 32% by their $M_n$s and to be 30% by eq 7, close to the feed ratio of 32% that was calculated using St of 1.49 g and PIsM of 0.70 g. The PIs composition distribution against the elution volume was found to be narrow, as shown in Figure 3. We succeeded in preparing a $(PIs)_{6.6}$-*star*-$(PSt)_1$ star block copolymer having a narrow molecular weight distribution and a narrow composition distribution using the PIsM macromonomer.

**Preparation of Star Block Copolymers of $(B)_1$-*star*-$(A)_n$.** In this section, the second approach is discussed, namely, the polymerization of the monomers followed by copolymerization of the corresponding macromonomers. Two synthetic routes using PStM and PIsM macromonomers were as follows, and the polymerization conditions are shown in Table 2.

$$\text{Is} + s\text{-BuLi} \rightarrow (\text{PIs})_1^- \tag{12}$$

$$(\text{PIs})_1^- + n\text{PStM} \rightarrow (\text{PIs})_1\text{-}star\text{-}(\text{PSt})_n \tag{13}$$

$$\text{St} + s\text{-BuLi} \rightarrow (\text{PSt})_1^- \tag{14}$$

$$(\text{PSt})_1^- + n\text{PIsM} \rightarrow (\text{PSt})_1\text{-}star\text{-}(\text{PIs})_n \tag{15}$$

In eq 12, PIs was prepared by *s*-BuLi using a common technique, and then Bz solution of PStM was added to the PIs polymerization solution, as shown in eq 13. The polymerization solution gradually changed from colorless to red. The solutions maintained a red color during the copolymerization. As shown in Figure 4, the GPC peak strength of PIs decreased, and a new GPC peak appeared at a higher $M_n$ side that corresponded to the $(PIs)_1$-*star*-$(PSt)_n$ star block copolymer. Because some of the $PIs^-$ carbanions were deactivated by impurities contained in the PStM solution, the final product contained a mixture of $(PIs)_1$-*star*-$(PSt)_n$ and PIs. All of the PStM molecules for which GPC peak appeared at an elution volume of 31.5 mL were polymerized to produce $(PIs)_1$-*star*-$(PSt)_n$ in 100% yield. As shown in Table 5, it takes 30 min for the PStM macromonomer to be initiated by the $PIs^-$ carbanions, and the $M_n$ values of the resultant $(PIs)_1$-*star*-$(PSt)_n$ increase with an increase in polymer yields. The $M_w/M_n$ value of $1.1_1$ for the final product is larger than that of $1.0_3$ for the PIs.

Attention should be directed to the PIs composition distribution of the resultant $(PIs)_1$-*star*-$(PSt)_n$ star block copolymer. As shown in Figure 4, the PIs contents are not constant among the elution volume but decrease with a decrease in the elution volume; namely, the higher the $M_n$ of $(PIs)_1$-*star*-$(PSt)_n$, the lower the PIs contents.

The copolymerization would be inhomogeneously performed with a tapered copolymerization rate. This copolymerization is not a typical case in which a macromolecular initiator reacts with an other monomer, but a special case in which the $PIs^-$ macromolecular initiator reacts with the PStM macromonomer. It should take a long time for the $PIs^-$ carbanions to initiate PStM due to the repulsive interaction between PIs chains and

**Table 4. Molecular Characteristics of $(PIs)_n$ Star Polymers[a] and $(PIs)_n$-*s*-$(PSt)_1$ Star Block Copolymer[a]**

| | | $10^{-4}M_n$ | | $M_w/M_n$ | | | | | $w^{PIs}$/%[e] | |
|---|---|---|---|---|---|---|---|---|---|---|
| polymers | *t* (h) | GPC | LALLS[b] | GPC | LALLS[b] | arms[c] | yield/% PIsM | $f_I$[d] | $M_n$ | $\sum w_i^{PIs}$ |
| $(PIs)_{3.0}$ | 0.2 | $1.3_7$ | $1.5_8$ | $1.0_3$ | $1.0_6$ | 3.0 | 45 | 0.28 | | |
| $(PIs)_{5.5}$ | 0.4 | $1.8_8$ | $2.8_7$ | $1.1_1$ | $1.0_8$ | 5.5 | 84 | 0.28 | | |
| $(PIs)_{6.2}$ | 1.1 | $2.0_8$ | $3.2_0$ | $1.1_0$ | $1.0_5$ | 6.2 | 93 | 0.28 | | |
| $(PIs)_{6.6}$ | 4.5 | $2.0_8$ | $3.4_2$ | $1.1_1$ | $1.0_4$ | 6.6 | 99 | 0.27 | | |
| $(PIs)_{6.6}$-*s*-$(PSt)_1$[f] | 17 | $6.5_8$ | $10._8$ | $1.0_8$ | $1.0_4$ | | 100[g] | 1.00[g] | 32 | 30 |

[a] Prepared by *sec*-BuLi in Bz at room temperature under a pressure of $10^{-6}$ mmHg. [b] A special analysis using GPC equipped with low-angle laser light-scattering.[23] [c] The degree of polymerization of the $(PIs)_n$ star polymers. [d] Initiation efficiency determined by $M_k/M_n$. [e] PIs contents determined by $M_n^{PIs}/M_n^{block}$ and by GPC using UV and RI detectors. [f] $M_n = (5.1_9 \times 10^3\ g\ mol^{-1}) \times 6.6_0 + (7.3_8 \times 10^4\ g\ mol^{-1}) = 10._8 \times 10^4\ g\ mol^{-1}$. [g] Determined for the second monomer of St.

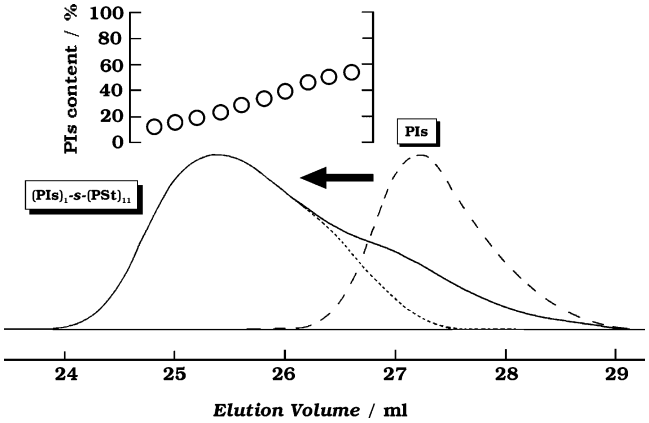


**Figure 4.** GPC chromatograms of PIs and $(PIs)_1$-*s*-$(PSt)_{11}$ star block copolymer. The final product was purified by repeated dissolution−reprecepitation, and the resultant GPC chromatogram of $(PIs)_1$-*s*-$(PSt)_{11}$ is also shown as a broken curve.

PStM chains. In contrast, it should require a short period of time for the $(PIs)_1$-*star*-$(PSt)_m^-$ carbanions to propagate PStM due to the weaker repulsive interaction between $(PIs)_1$-*star*-$(PSt)_m^-$ and PStM. The copolymerization rate should be accelerated by the PSt content of the growing $(PIs)_1$-*star*-$(PSt)_m^-$; namely, inhomogeneous copolymerization was performed. Therefore, the final product of $(PIs)_1$-*star*-$(PSt)_n$ has a broad molecular weight distribution and also shows higher PIs contents at its lower $M_n$ sides and lower PIs contents at its higher $M_n$ sides.

As the reviewer of the present paper pointed out, another approach is possible: namely, a slow initiation reactivity of $(PIs)_1^-Li^+$ to PStM in eq 13 rather than that of $(PSt)_1^-Li^+$ to PIsM having a styryl group in eq 15. It is well-known that the addition of St monomer to $PIs^-Li^+$ is slower than that of St to $PSt^-Li^+$, and hence the process described by eq 13 can be regarded as polymerization with slow initiation. However, we had also known that the $M_w/M_n$ values of PSt-*block*-PIs and PIs-*block*-PSt block copolymers are probably the same as that of PSt, and their values are less than $1.0_5$.[25] The sequence of addition of Is and St monomers is not a dominant factor in affecting the $M_w/M_n$ values of the resultant block copolymers, even though the anionic reactivity of Is is lower than that of St. In contrast, the $M_w/M_n$ values of PSA-*block*-PSt and PSt-*block*-PSA were $1.0_5$ and $1.2_5$, respectively, where PSA is poly(secondary aminostyrene).[26] When the anionic reactivity of SA is much lower than that of St, the sequence of addition of SA and St is capable of affecting the $M_w/M_n$ values. Therefore, the slow initiation reactivity of $PIs^-Li^+$ to the styryl group of PStM in eq 13 does not seem to be a dominant factor of the inhomogeneous copolymerization of $(PIs)_1$-*star*-$(PSt)_n$.

These would be perhaps the simple explanation to account for the preparation of the tapered polymers of $(PIs)_1$-*star*-$(PSt)_n$. The important fact is that this synthetic route is not suitable for preparing the $(PIs)_1$-*star*-$(PSt)_n$ star block copolymers having a narrow PIs composition distribution. Similarly, the synthetic route of (15) would not be suitable for preparing the $(PSt)_1$-*star*-$(PIs)_n$ star block copolymers having a narrow molecular weight distribution and a narrow PIs composition distribution. Therefore, the details of the synthetic route of (15) are not described in the present paper.

**Initiation Efficiency.** The initiation efficiency ($f_I$) can be determined using the ratio $M_n/M_k$, where $M_k$ is calculated by the amounts of monomer and initiator. The $f_I$ is one of the most important characteristics when discussing a living mechanism.[18,27] When the $f_I$ value is kept to 1.0 in a polymer yield of 0−100%, the polymerization is performed by the living mechanism. However, even if the polymerization is performed by the living mechanism, it is common for the $f_I$ value to be less than 1.0 because (i) some of the initiators are deactivated by impurities contained in the polymerization solution at the initial stage of polymerization or (ii) some of the initiators are deactivated by the glass surface of the ampule when the initiators are kept in a refrigerator for a long time before polymerization. It is important that even if the $f_I$ value is less than 1.0, livingness should keep the $f_I$ value constant in a polymer yield of 0−100%.

As shown in Tables 3 and 4, the synthetic routes of (9) for Is polymerization, (11) for the St one, and (12) for the Is one show $f_I$ values of 1.00. These results indicate that their polymerizations are carried out by a living mechanism, as expected for an ideal anionic living polymerization. On the other hand, the synthetic route (8) of PStM polymerization shows $f_I$ values of 0.62−0.60 for polymerization times of 0.4−4.6 h. The synthetic route (10) of PIsM polymerization shows $f_I$ values of 0.28−0.27 for 0.2−4.5 h. The synthetic route (13) of PStM polymerization shows $f_I$ values of 0.35−0.32 for 0.5−150 h. These three results also indicate the living mechanism for anionic polymerization of PStM and PIsM macromonomers in Bz by *s*-BuLi.

Next, to further clarify the livingness of the macromonomers, we will discuss the difference in the $f_I$ values of their polymerization. Since the $f_I$ value for polymerizing Is is 1.0 (Table 5), it was found that (ii) some of the initiators were not deactivated by being kept in a refrigerator for a long time before polymerization. The reason that the $f_I$ values were less than 1.0 is that (i) some of the initiators were deactivated by impurities contained in the polymerization solution at an initial stage of polymerization. Hence, purification of the macromonomers using PPBNa should be discussed.

The $f_I$ values depend on the time of purging before polymerization and the amounts of initiator used in the polymerization, as shown in Figure 5. It is easily understood that the $f_I$ values increase with an increase in the purging time. However, it is necessary to explain why the $f_I$ values depend on the amounts of initiator. The amount of impurities contained in the

**Table 5. Molecular Characteristics of PIs[a] and $(PIs)_1$-*s*-$(PSt)_n$[a] Star Block Copolymers**

| | | $10^{-4}M_n$ | | $M_w/M_n$ | | | | | $w^{PIs}$ /%[e] | |
|---|---|---|---|---|---|---|---|---|---|---|
| polymers | *t* (h) | GPC | LALLS[b] | GPC | LALLS[b] | arms[c] | yield/% Is | $f_I$[d] | $M_n$ | $\sum w_i^{PIs}$ |
| PIs | 18 | $2.1_7$ | $1.5_8$ | $1.1_6$ | $1.0_3$ | | 100 | 1.00 | | |
| $(PIs)_1$-*s*-$(PSt)_n$ | $18._5$ | | | | | | 3[f] | | | |
| $(PIs)_1$-*s*-$(PSt)_{9.5}$ | $30._5$ | $4.1_7$ | $6.7_8$ | $1.1_3$ | $1.3_0$ | 9.5 | 96[f] | 0.35[f] | 23 | 32 |
| $(PIs)_1$-*s*-$(PSt)_{11}$[g] | 88 | $4.2_1$ | $7.4_9$ | $1.1_3$ | $1.1_1$ | 11 | 100[f] | 0.32[f] | 21 | 30 |

[a] Prepared by *sec*-BuLi in Bz at room temperature under a pressure of $10^{-6}$ mmHg. [b] A special analysis using GPC equipped with low-angle laser light-scattering.[23] [c] The degree of polymerization of the $(PSt)_n$ star polymers. [d] Initiation efficiency determined by $M_k/M_n$. [e] PIs contents determined by $M_n^{PIs}/M_n^{block}$ and by GPC using UV and RI detectors. [f] Determined for the second monomer of PStM. [g] $M_n = (1.5_8 \times 10^4\ g\ mol^{-1}) + (5.4_5 \times 10^3\ g\ mol^{-1}) \times 10._8 = 7.4_9 \times 10^4\ g\ mol^{-1}$.

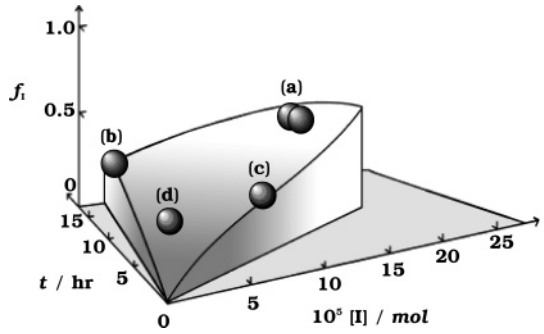


**Figure 5.** Initiation efficiency ($f_I$) plotted against the purging time (*t*) using PPBNa and the amount of initiator ([I]): (a) $(PSt)_{4.7-6.1}$ in Table 3, (b) $(PIs)_{3.0-6.6}$ in Table 4, (c) $(PIs)_1$-*s*-$(PSt)_{9.5-11}$ in Table 5, and (d) $(PSt)_{8.7-12}$ star polymers using PStM reported elsewhere.[18]

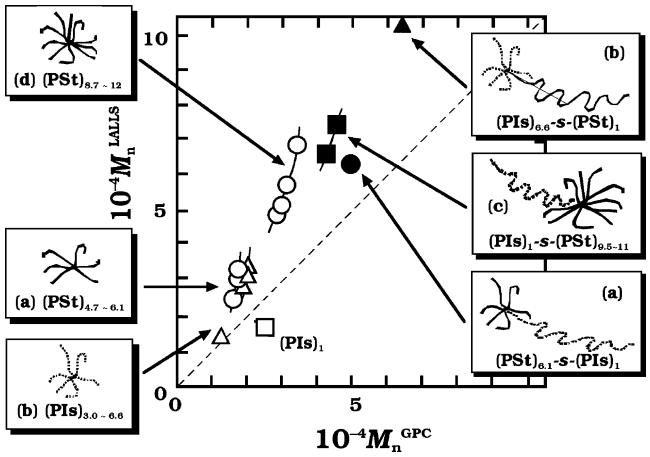


**Figure 6.** Relationships between $M_n^{LALLS}$ values determined by GPC-LALLS and $M_n^{GPC}$ values determined using standard PSts: (a) $(PSt)_{4.7-6.1}$ and $(PSt)_{6.1}$-*s*-$(PIs)_1$ in Table 3, (b) $(PIs)_{3.0-6.6}$ and $(PIs)_{6.6}$-*s*-$(PSt)_1$ in Table 4, (c) $(PIs)_1$-*s*-$(PSt)_{9.5-11}$ in Table 5, and (d) $(PSt)_{8.7-12}$ star polymers using PStM reported elsewhere.[18]

macromonomers before purification is proportional not only to their weight but also to their surface area. In addition, some impurities had been attached to the surface inside of the ampules in which the macromonomers were freeze-dried at the first stage of the purification of the macromonomer. Therefore, the $f_I$ values decrease with a decrease in the amounts of initiator.[27] This fact is a fundamental answer to the question of why it is difficult to polymerize the macromonomers having a $f_I$ value of 1.0. In common polymerization of St and Is, monomers of 10−20 g were polymerized; however, in the macromonomers' polymerization, macromonomer of 1−2 g were polymerized because many difficulties arose in their synthesis. The larger-scale polymerization shows the higher $f_I$ values, even if the deactivation of the initiators occurred via the same mechanism.

As shown in Figure 5, by the greater purging time and greater amounts of initiator, the $f_I$ values should reach 1.0 in Bz by *s*-BuLi at room temperature for a nonpolar solvent system. As we had discussed elsewhere, the $f_I$ values were 0.98 when polymerizing PStM to prepare the star polymers in THF by *n*-BuLi at −78 °C for a polar solvent system.[18] The purging reagent of PPBNa can deactivate the impurities in THF rather than those in Bz because of a strong affinity of sodium carbanions of PPBNa for THF rather than that for Bz. In conclusion, the anionic living polymerization of the PStM and PIsM macromonomers was confirmed by the fact that $f_I$ was constant despite the increase of the polymer yields when the macromonomers were sufficiently purified with PPBNa as a purging reagent.

**Specific Dimensions of the $(A)_n$ Star Polymers and $(A)_n$-*star*-$(B)_1$ Star Block Copolymers.** Attention should be directed to the molecular structure or a specific dimension of the $(A)_n$ star polymers and $(A)_n$-*star*-$(B)_1$ star block copolymers in THF. For this purpose, light-scattering measurements must be performed to determine the relationship between $M_w$ and a mean-square radius of gyration $\langle S^2 \rangle$ of the samples. Though a detailed study will be carried out in the future, a brief discussion of a specific dimension of the samples in THF follows.

Two molecular weights of all samples prepared in the present study were simultaneously determined: one was the absolute molecular weight ($M_n^{LALLS}$) determined by LALLS using a special analysis, and the other was the polystyrene-reduced molecular weight ($M_n^{GPC}$) determined by a common GPC technique using standard polystyrenes. The $M_n^{LALLS}$ values were plotted against the $M_n^{GPC}$ values, as shown in Figure 6. Schematic molecular structures were also inserted in the corresponding plots. A linear broken line with a slope of 1.0 corresponds to the plots of $M_n^{LALLS}$ against $M_n^{GPC}$ for the linear PSt. The polymers that appear in the upper region above the broken line have chain dimensions that are contracted rather than chain dimensions of the linear PSt.

On the other hand, the $M_n^{GPC}$ values correspond to the dimensions of the polymers in THF as a result of the mechanism of the GPC measurements. Hence, the $M_n^{GPC}{}_{star}/M_n^{LALLS}{}_{star}$ ratios might correspond to the specific volume ($\upsilon_s^{star}$) of the samples in THF:[18,28]

$$\upsilon_s^{star} = M_n^{GPC}{}_{star}/M_n^{LALLS}{}_{star} \tag{16}$$

In the case of linear PSt, linear PIs, and linear poly(*n*-hexyl isocyanate)s (PHIC), the $M_n^{GPC}/M_n^{LALLS}$ ratios were determined by GPC-LALLS as 1.0, 0.8, and 1.9, respectively.[18,28] The higher value for the PHIC reflects the bulkiness of the rodlike polymer.[29]

The $\upsilon_s^{star}$ values of $(A)_n$ and $(A)_n$-*star*-$(B)_1$ are plotted against the number of arms (*n*). As compared with the constant $M_n^{GPC}/M_n^{LALLS}$ values of linear PSt, PMMA, and PHIC polymers, the $\upsilon_s^{star}$ values decreased with an increase in the number of arms (*n*) (Figure 7). This behavior reflects the structure of star polymers. In the case of regular comb-shaped homopolymers

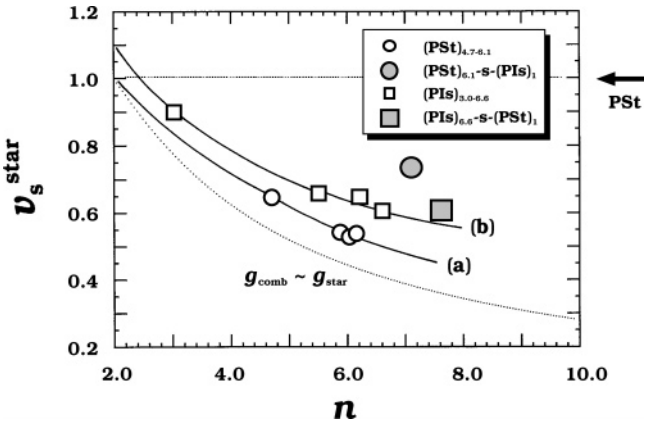


**Figure 7.** Plots of $\upsilon_s^{star}$ against the number of arms ($n$): (a) $(PSt)_{4.7-6.1}$ and $(PSt)_{6.1}$-*s*-$(PIs)_1$ in Table 3 and (b) $(PIs)_{3.0-6.6}$ and $(PIs)_{6.6}$-*s*-$(PSt)_1$ in Table 4. The calculated $g_{star}$ curve of a regular star polymer is also plotted in the figure.

at a $\theta$ state, a mean-square radius of gyration $\langle S^2\rangle_{comb}$ can be derived (for large $m$) as[30,31]

$$\langle S^2\rangle_{comb} = [1 + (1 - \lambda)^{7/3}(3n - 2)/n^2](mb^2/6) \quad (17)$$

Therefore, for regular comb-shaped and linear polymers with the same $m$ and $b$ at a $\theta$ state

$$g_{comb} = \langle S^2\rangle_{comb}/\langle S^2\rangle_{linear} = [\lambda + (1 - \lambda)^{7/3}(3n - 2)/n^2] \quad (18)$$

where $m$ and $b$ are the degree of polymerization of the comb chain and the bond length, respectively; $\langle S^2\rangle_{linear}$ is the mean-square radius of gyration for a linear polymer chain, and $\lambda$ and $n$ are the fraction of mass in the backbone and the number of branches, respectively. The term $(3n - 2)/n^2$ is well-known to be a $g_{star}$ value of a regular star polymer. The $g_{comb}$ value estimated from eq 18 may be considered as a measure of branching.

In the case of the $(PSt)_n$ star polymers, $\lambda$ can be estimated as 0.019 ($= 104$ g mol$^{-1}$/(5450 − 104) g mol$^{-1}$). From eq 18, the $g_{comb}$ value became equal to the $g_{star}$ value with an error of less than 3.5% in a range of $n = 2-10$. Therefore, the $g_{comb}$ can be converted as follows: $g_{comb} = g_{star} = \langle S^2\rangle_{star}/\langle S^2\rangle_{linear} = \upsilon_s^{star}/\upsilon_s^{linear} = \upsilon_s^{star}$ due to $\upsilon_s^{linear} = 1$, where $\upsilon_s^{linear}$ is a specific volume of the linear PSt. In the case of the $(PSt)_n$-*star*-$(PIs)_1$ star block copolymers, the $g_{star\ block}$ value was not derived in the form of an exact equation. As a first approximation, a PIs chain of $(PSt)_n$-*star*-$(PIs)_1$ can be considered as a main chain, and the PSt arms can be considered as comb chains, although the comb chains (PSt chains) are different from a main chain (a PIs chain) and the comb chain points have a localized distribution on the main chain. Hence, the $\lambda$ of $(PSt)_{6.1}$-*star*-$(PIs)_1$ can be estimated as 0.48 in the same manner as for the PIs weight fraction ($3.0_7 \times 10^4$ g mol$^{-1}$ for $M_n$ of $(PIs)_1$/$3.3_2 \times 10^4$ g mol$^{-1}$ for $M_n$ of $(PSt)_n$). From eq 18, the $g_{comb}$ value became equal to the $g_{star}$ value with an error of less than 9.6% for an $n$ value of more than 5. Therefore, the $g_{comb}$ can be converted as follows: $g_{comb} = g_{star} = \langle S^2\rangle_{star}/\langle S^2\rangle_{linear} = \upsilon_s^{star}/\upsilon_s^{linear} = \upsilon_s^{star}$. Therefore, we have

$$\upsilon_s^{star} = (3n - 2)/n^2 \quad (19)$$

The $\upsilon_s^{star}$ value can be calculated as a function of $n$. As shown in Figure 7, the observed $\upsilon_s^{star}$ curve can be qualitatively explained by eq 19. However, there are gaps among the three curves. The observed curve of $(PIs)_n$ is parallel to that of $(PSt)_n$, where this gap might attribute to the difference in the $\upsilon_s^{star}$ values between 1.3 of PIs (at $n = 1$) and 1.0 of PSt. On the other hand, the two observed curves are also different from the calculated curve. These gaps are attributed to the fact that the theoretical $\upsilon_s^{star}$ value can be derived at a $\theta$ state and the fact that the observed $\upsilon_s^{star}$ values can be determined in a good solvent of THF. To achieve a quantitative fit between the three curves, detailed experiments should be carried out at a $\theta$ state.

As shown in Figure 7, the observed $\upsilon_s^{star}$ values of the two star block copolymers shifted from the corresponding curves of the star polymers. In the case of $(PSt)_{6.1}$-*star*-$(PIs)_1$, a PIs chain has 5.6 times higher $M_n$ value than that of a PSt chain, and this factor tends to increase the $\upsilon_s^{star}$ value from that of $(PSt)_{7.1}$. The PIs chain exhibits the higher $\upsilon_s^{star}$ value than that of the PSt chain due to the $\upsilon_s^{star}$ value of PIs is 1.3. Both factors are positive and hence are responsible to a big gap in the $\upsilon_s^{star}$ value between the star polymers and star block copolymer. In the case of $(PIs)_{6.6}$-*star*-$(PSt)_1$, a PSt chain has 14 times higher $M_n$ value than that of a PIs chain, and this factor tends to increase the $\upsilon_s^{star}$ value from that of $(PIs)_{7.7}$. The PSt chain exhibits the lower $\upsilon_s^{star}$ value than that of the PIs chain due to the $\upsilon_s^{star}$ value of PSt is 1.0. Both factors are negative and hence are responsible to a small gap in the $\upsilon_s^{star}$ value between the star polymers and star block copolymer. The qualitative explanation mentioned above might be correct; however, it is difficult to carry out quantitative analysis of the $\upsilon_s^{star}$ values of the star block copolymers in the present paper. We are planning more systematic measurements using dynamic and static light-scattering techniques on the star block copolymers.

When plotting $\upsilon_s^{star}$ against $n$ in Figure 7, the average numbers of arms were used for $(PSt)_n$ and $(PIs)_n$. However, a distribution in number of arms is very important to discuss solution properties discussed in this section and also to discuss asymmetric effect on the morphology formation in bulk discussed in the next section. PStM and PIsM have molecular weight distributions ($M_w/M_n < 1.0_4$), and $(PSt)_n$ and $(PIs)_n$ have also molecular weight distributions ($M_w/M_n < 1.1_5$). It seems difficult to estimate the distribution in number of arms at the present stage. We are planning to estimate the distribution in number of arms using recent analytical technique such as MALDI-TOF mass spectrometry for systematic solution properties of star polymers and star block copolymers.

**Morphology.** Two $(A)_n$-*star*-$(B)_1$ star block copolymers were prepared in a 100% yield. However, the coupling efficiency of PIsM macromonomer was not 100%. Further, when obtaining the precursors of the $(A)_n$ star polymers in a process of macromonomer polymerization, the ampules of precursors were sealed off by flame. Even if the polymers adhering to the glass surface were washed with Bz, small amounts of polymers might be decomposed to produce impurities when sealing off by flame. A small amount of the $(A)_n^-$ carbanions could have been deactivated by these impurities. Therefore, the final product contained $(A)_n$-*star*-$(B)_1$ as a main product (more than 95 wt %), and contained $(A)_n$ and A as byproducts (less than 5 wt %). Removal of $(A)_n$ and A from the final product is necessary to obtain $(A)_n$-*star*-$(B)_1$.

In the case of $(PSt)_{6.1}$-*star*-$(PIs)_1$, 1-propanol (22 g) was added to the cyclohexane solution (30 g) of the final product (1.1 g) to precipitate $(PSt)_n$ and PSt. $(PSt)_{6.1}$-*star*-$(PIs)_1$ was obtained from the solution in an 88% yield. In the case of $(PIs)_{6.6}$-*star*-$(PSt)_1$, 1-propanol (4 g) was added to the heptane solution (7 g) of the final product (1.0 g) to precipitate $(PIs)_{6.6}$-*star*-$(PSt)_1$. $(PIs)_n$ and PIs exist in the solution. This procedure was done

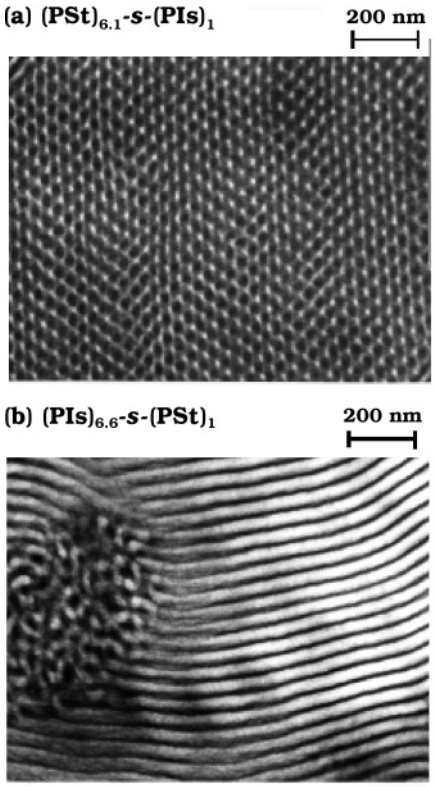


**Figure 8.** Transmission electron micrographs of (a) $(PSt)_{6.1}$-*s*-$(PIs)_1$ and (b) $(PIs)_{6.6}$-*s*-$(PSt)_1$ star block copolymer films, which were cast from the respective THF solutions and were subsequently stained with $OsO_4$. White and black regions correspond to PSt and PIs phases, respectively.

twice to obtain $(PIs)_{6.6}$-*star*-$(PSt)_1$ in a 74% yield. The purification results were tested by GPC.

Thin films of each of the two samples of $(PSt)_{6.1}$-*star*-$(PIs)_1$ and $(PIs)_{6.6}$-*star*-$(PSt)_1$ cast from their THF solutions were dried under a vacuum at 40 °C for 2 days. To further promote the formation of equilibrium morphologies, the films were annealed at 70 °C for 1 day. Figure 8 shows electron micrographs of the two films. The black and white regions in the electron micrographs correspond to the PIs phase and PSt phase, respectively. The two samples formed clear microphase-separated (MS) structures.

The $(PSt)_{6.1}$-*star*-$(PIs)_1$ film has a PIs content of 48 wt % (52 vol %). A linear block copolymer that has one composition at 52 vol % is expected to form a lamellar structure.[5] However, the $(PSt)_{6.1}$-*star*-$(PIs)_1$ film showed a spherical structure of PIs, wherein PSt formed a continuous phase. A more detailed explanation of Figure 8a is that hexagonally domain packing manner can be conceived and furthermore three contrasts can be recognized. It is dangerous to assign the morphology of Figure 8a as a spherical structure, and hence X-ray scattering experiment that is in progress is required for the assignment. However, bicontinuous phases in two-dimensional or three-dimensional structures are omitted from the present discussion due to being complicated. As a simple discussion of the morphological transition of the star block copolymers, we assign the morphology of Figure 8a as a spherical structure.

The $(PIs)_{6.6}$-*star*-$(PSt)_1$ film contains PIs of 32 wt % (35 vol %). A linear block copolymer that has one composition in an amount of 35 vol % is expected to form a lamellar structure or a cylinder structure of PIs. However, the $(PIs)_{6.6}$-*star*-$(PSt)_1$ film showed a lamellar structure or a cylinder structure of PSt. In conclusion, the morphology of $(A)_n$-*star*-$(B)_1$ tends to shift to the higher star polymer (A arms) content side of the morphological transition line for the linear block copolymers expected by Molau.[5]

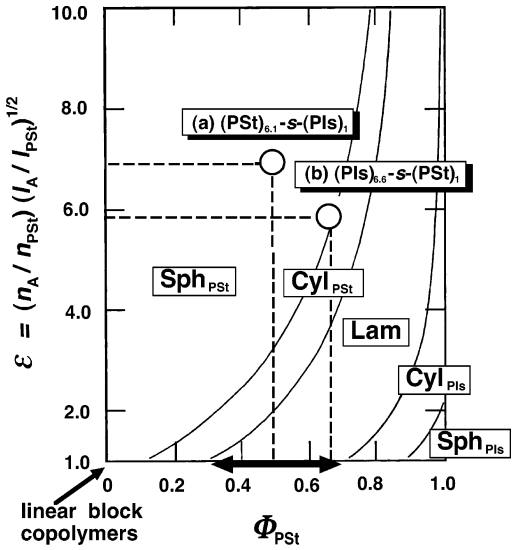


**Figure 9.** Theoretical phase diagram of (a) $(PSt)_{6.1}$-*s*-$(PIs)_1$ and (b) $(PIs)_{6.6}$-*s*-$(PSt)_1$ star block copolymer films calculated by Milner, where the bicontinuous phases are omitted due to being complicated. Symbols represent the MS structures of $Sph_{PSt}$ (spheres of PSt), $Cyl_{PSt}$ (cylinders of PSt), Lam (lamella), $Cly_A$ (cylinders of A polymer), and $Sph_A$ (spheres of A polymer). Bold outlined symbols indicate the two samples characterized in this study.

The morphological behavior of $(A)_n$-*star*-$(B)_1$ may be rationalized by considering of the film-casting process from a dilute polymer solution. Since an MS structure will develop when the concentration of the polymer solution attains a critical concentration, the morphology should be determined by the apparent volume fraction.[32,33] The apparent volume fraction of $(A)_n$ to $(B)_1$ at the critical concentration should be much larger than the corresponding real volume fraction. One of the reasons for this is that the arm chain of the $(A)_n$ star polymer extends rather more than the corresponding unperturbed polymer chain due to the arm chains becoming crowded near the center of star polymers. Therefore, the $(A)_n$-*star*-$(B)_1$ star block copolymer is believed to form a characteristic MS structure that is distinct from that of the linear block copolymer.

The MS structures of block copolymers with nonlinear architectures have been the focus of a considerable amount of recent work. One of the representative works is a series of mikto-arm star block copolymers $(A_mB_n)$[34,35] and model graft copolymers[2,3] prepared using anionic polymerization and controlled chlorosilane chemistry. Gido and co-workers have reported that the MS structures shifted to structures having higher volume fractions of the higher arm number component, as compared with the structures of linear block copolymers.[34,35] This behavior is qualitatively similar to that observed in the present study. Milner has quantitatively calculated a shift of the morphological transition lines as a function of a volume fraction of component B ($\phi_B$) and a molecular asymmetry parameter ($\epsilon$).[36,37]

$$\epsilon = (n_A/n_B)(l_A/l_B)^{1/2} \tag{20}$$

Here, $n_A$ and $n_B$ are the numbers of arms of $(A)_m$-*star*-$(B)_n$, and $l_i = V_i/\langle S_i^2\rangle = v_i/b_i^2$. $V_i$ and $\langle S_i^2\rangle$ are the volume and the mean-square radius of gyration of one arm of polymer $i$, respectively, while $v_i$ is the segmental volume and $b_i$ is the statistical segment length of component $i$.

$(PSt)_{6.1}$-*star*-$(PIs)_1$ and $(PIs)_{6.6}$-*star*-$(PSt)_1$ can be considered to be an asymmetric mikto-arm star block copolymer. Using $v_{PIs} = 0.132$ nm$^3$ and $b_{PIs} = 0.68$ nm for PIs, and $v_{PSt} = 0.176$ nm$^3$ and $b_{PSt} = 0.69$ nm for PSt, the $(l_{PIs}/l_{PSt})^{1/2}$ of 0.878 is calculated.[20] Hence, asymmetry parameters of $\epsilon$ are 7.0 for $(PSt)_{6.1}$-*star*-$(PIs)_1$ ($n_A = 6.1$, $n_B = 1.0$) and 5.8 for $(PIs)_{6.6}$-*star*-$(PSt)_1$ ($n_A = 6.6$, $n_B = 1.0$). Figure 9 shows the mapping of the morphological results of the two samples onto the theoretical phase diagram calculated by Milner. The shifts of the MS structures from those of the corresponding linear block copolymers are explained quantitatively by the asymmetric factor.

## Conclusion

We successfully produced $(PSt)_{6.1}$-*star*-$(PIs)_1$ and $(PIs)_{6.6}$-*star*-$(PSt)_1$ star block copolymers; namely, each of the PStM and PIsM macromonomers that were purified by a PPBNa-purging reagent under a pressure of $10^{-6}$ mmHg was first anionically polymerized by a living mechanism, and then each of the corresponding monomers was sequentially copolymerized. In contrast, the synthetic route by which the $PIs^-$ carbanions copolymerize PStM was found to be unsuitable for preparing $(PIs)_1$-*star*-$(PSt)_n$ having a narrow molecular weight distribution and a narrow PIs composition distribution. The living mechanism of the macromonomers polymerization was confirmed by the fact that their $f_I$ values remained constant through the process of polymerization.

The specific dimensions of $v_s^{star}$ calculated by $M_n^{GPC}{}_{star}/M_n^{LALLS}{}_{star}$ for the $(A)_n$ star polymers and the $(A)_n$-*star*-$(B)_n$ star block copolymers were qualitatively explained by a model of regular comb-shaped polymers. A film of $(PSt)_{6.1}$-*star*-$(PIs)_1$ having 48 wt % of PIs shows a spherical structure of PIs, and a film of $(PIs)_{6.6}$-*star*-$(PSt)_1$ having 33 wt % of PIs shows a cylinder structure of PSt. The morphology tends to shift to the higher star polymer content side of the morphological transition line of linear block copolymers expected by Molau. This interesting gap in the morphology between the $(A)_n$-*star*-$(B)_1$ star block copolymers and the A-*block*-B linear block copolymers was quantitatively explained by a volume fraction and an asymmetric factor proposed by Milner.

**Acknowledgment.** We are deeply indebted to Mr. K. Hasegawa, Electronic Materials Department, Electronic Materials Division, JSR Corp., Tokyo, Japan, for his preparation of the electron micrographs.

## References and Notes

(1) Hadjichristidis, N. *Adv. Polym. Sci.* **1999**, *142*, 71.
(2) Se, K.; Yamazaki, H.; Shibamoto, T.; Takano, A.; Fujimoto, T. *Macromolecules* **1997**, *30*, 1570.
(3) Se, K.; Miyawaki, K.; Hirahar, K.; Takano, A.; Fujimoto, T. *J. Polym. Sci., Polym. Chem.* **1998**, *36*, 3021.
(4) Chen, J. T.; Thomas, E. L.; Ober, C. K.; Mao, G.-p. *Science* **1996**, *273*, 343.
(5) Hamley, I. W. *The Physics of Block Copolymers*; Oxford Sci. Publ.: Oxford, 1998.
(6) Li, Z.; Hillmyer, M. A.; Lodge, T. P. *Macromolecules* **2004**, *37*, 8933.
(7) Li, Z.; Hillmyer, M. A.; Lodge, T. P. *Macromolecules* **2006**, *39*, 765.
(8) Tsukahara, Y.; Namba, S.; Iwasa, J.; Nakano, Y. Kaeriyama, K. Takahisa, M. *Macromolecules* **2001**, *34*, 2624.
(9) Hokajo, T.; Terao, K.; Nakamura, Y.; Norisuye, T. *Polym. J.* **2001**, *33*, 481.
(10) Nakamura, Y.; Norisuye, T. *Polym. J.* **2001**, *33*, 874.
(11) Ito, K. *Prog. Polym. Sci.* **1998**, *23*, 581.
(12) Ishizu, K.; Uchida, S. *Prog. Polym. Sci.* **1999**, *24*, 1439.
(13) Pantazis, D.; Chalari, I.; Hadjichristidis, N. *Macromolecules* **2003**, *36*, 3783.
(14) Vazaios, A.; Hadjichristidis, N. *J. Polym. Sci., Part A: Polym. Chem.* **2005**, *43*, 1038.
(15) Knauss, D. M.; Huang, T. *Macromolecules* **2003**, *36*, 6036.
(16) Se, K.; Suzuki, M.; Matsuo, T.; Umeda, T.; Ueno, M. *Kobunshi Ronbunshu (Jpn. J. Polym. Sci. Technol.)* **1992**, *49*, 817.
(17) Se, K.; Suzuki, M. *Rep. Prog. Polym. Phys. Jpn.* **1993**, *36*, 491.
(18) Se, K.; Inoue, N.; Yamashita, M. *Polymer* **2005**, *46*, 9753.
(19) Se, K.; Matsumura, K.; Kazama, T.; Fujimoto, T. *Polym. J.* **1997**, *29*, 434.
(20) Se, K. *Prog. Polym. Sci.* **2003**, *28*, 583.
(21) Senoo, K.; Endo, K. *J. Polym. Sci., Part A: Polym. Chem.* **2000**, *38*, 1241.
(22) Merrifield resin was purchased from Peptide Institute Inc., 4-1-2 Inc., Minoh-Shi, Osaka 562−8686, Japan (http://www.peptide.co.jp).
(23) Se, K.; Sakakibara, T.; Ogawa, E. *Polymer* **2002**, *43*, 5447.
(24) Se, K.; Aoyama, K.; Aoyama, J.; Donkai, M. *Macromolecules* **2003**, *36*, 5878.
(25) Funabashi, H.; Miyamoto, Y.; Isono, Y.; Fijimoto, T.; Matsushita, Y.; Nagasawa, M. *Macromolecules* **1983**, *16*, 1.
(26) Se, K.; Kudoh, S. *J. Appl. Polym. Sci.* **1999**, *71*, 2039.
(27) Se, K.; Suzuki, M. *Kobunshi Ronbunshu* (*Jpn. J. Polym. Sci. Technol.*) **2000**, *57*, 851.
(28) Se, K.; Aoyama, K. *Polymer* **2004**, *45*, 79.
(29) Murakami, H.; Norisuye, T.; Fujita, H. *Macromolecules* **1980**, *13*, 345.
(30) Casassa, E. F.; Berry, G. C. *J. Polym. Sci., Part A-2* **1966**, *4*, 881.
(31) Casassa, E. F. Berry, G. C. Polymer Solution. In Allen, G., Ed. *Comprehensive Polymer Science*; Pergamon Press: New York, 1988; p 71.
(32) Hasegawa, H.; Tanaka, H.; Yamasaki, Y.; Hashimoto, T. *Macromolecules* **1987**, *20*, 1651.
(33) Helfand, E.; Wassermann, Z. R. *Macromolecules* **1980**, *13*, 994.
(34) Yang, L.; Hong, S.; Gido, S. P.; Velis, G.; Hadjichristidis, N. *Macromolecules* **2001**, *34*, 9069.
(35) Beyer, F. L.; Gido, S. P.; Uhrig, D.; Mays, J. W.; Tan, N. B.; Trevino, S. *J. Polym. Sci., Part B: Polym. Phys.* **1999**, *37*, 3392.
(36) Olmsted, P. D.; Milner, S. T. *Phys. Rev. Lett.* **1994**, *72*, 936.
(37) Olmsted, P. D.; Milner, S. T. *Macromolecules* **1998**, *31*, 4011.

MA061849O